

connect a fixed lightning source to a fixed spacecraft location at different frequencies. Similarly, various lightning sources may be connected to any fixed spacecraft position.

Tracing back the cone of possible ray paths from the spacecraft (distance $R = 6 R_J$; colatitude $= 90^\circ$) to Jupiter ($R = R_J$) with the conservative assumption of a half-angle of 10° for the cone leads to an acceptable source area at high latitudes with a radius of $\sim 16,000$ km, extending from 54°N to 79°N . This gives an area of $\sim 9 \times 10^8 \text{ km}^2$ in each hemisphere: we will consider only whistlers originating in the north polar regions because, at $6 R_J$, south polar whistlers pass through (and are greatly dispersed by) the Io plasma torus, and hence would appear different from the observed "fast" whistlers which have not traversed the torus. The whistler count rate of $\sim 0.12 \text{ sec}^{-1}$ corresponds to an occurrence frequency of $4 \times 10^{-3} \text{ km}^{-2} \text{ year}^{-1}$, very similar to the rate of optical flashes. Since lightning is normally associated with electrification processes due to the freezing of liquid droplets and is observed (2) to be associated with upwelling regions on Jupiter, the most reasonable locale for typical Jovian lightning discharges is in the water condensation region near 0°C and 6 bars. The water cloud layer, unlike the topmost NH_3 cloud layer, is expected to be optically thick (13), so that observations from above could reveal a higher frequency of whistlers than of optically visible flashes.

The lightning rate deduced from the whistler data is, of course, very imprecise. It could be argued that the interval of jovicentric distance over which whistlers were observed was so small that the true global average rate is much lower than the figure estimated above—that is, that lightning is associated only with a particular narrow latitude interval, or that only isolated regions of intense thunderstorm activity were present, making up no more than ~ 10 percent of the surface area of Jupiter. Alternatively, it could be argued that only a small fraction of the lightning discharges (say 10 percent or less) generate whistlers, and that the region of relatively intense activity is fairly representative of the rest of the planet. Thus an average lightning stroke rate as high as 4×10^{-2} or as low as $10^{-4} \text{ km}^{-2} \text{ year}^{-1}$ cannot be ruled out. Making the very generous assumption that every discharge generating a whistler is a "superbolt" dissipating about 10^{17} ergs, we could then have a total lightning energy dissipation rate as low as $3 \times 10^{-5} \text{ erg cm}^{-2} \text{ sec}^{-1}$. At the other

extreme, if 90 percent of the bolts are only of conventional size (10^{16} ergs) and are not detected because they are not large enough to generate whistlers, then extension of the high level of activity observed between 5.5 and $6.0 R_J$ to the entire surface of Jupiter would provide $3 \times 10^{-3} \text{ erg cm}^{-2} \text{ sec}^{-1}$. The conversion efficiency of convective energy into lightning is thus probably between 3×10^{-7} and 3×10^{-9} .

The whistler data, while difficult to interpret quantitatively, are reasonably consistent with the idea that the whistlers and the optical flashes are produced by the same population of discharges, dissipating $\sim 10^{-3} \text{ erg cm}^{-2} \text{ sec}^{-1}$ (efficiency, 10^{-7}). If further interpretation of the Voyager plasma-wave data leads to a higher estimate of the stroke rate, then we must conclude that most of the lightning occurs deep within the atmosphere, beneath the optically thick water cloud layer. The Voyager data do not provide any evidence for extensive lightning activity at high altitudes, near the NH_3 cloud tops; however, if all the observed flashes and whistlers were arbitrarily attributed to the NH_3 cloud region, the rate of energy dissipation by lightning and thunder would be only 10^{-4} of the rate of deposition of energy by ultraviolet photolysis of NH_3 and PH_3 in the same region.

A detailed treatment of the chemical consequences of lightning discharges in the Jovian atmosphere has appeared (14). For the present, it suffices to compare the energy fluxes available for each

of several competing processes for forming complex organic molecules and colored solids. This comparison, given in Table 1, demonstrates that known photochemical processes involving formation of inorganic chromophores are far more important than lightning-induced synthesis on Jupiter.

JOHN S. LEWIS

Department of Earth and Planetary Sciences, Massachusetts Institute of Technology, Cambridge 02139

References and Notes

1. B. A. Smith *et al.*, *Science* **204**, 951 (1979).
2. A. F. Cook, II, T. C. Duxbury, G. E. Hunt, *Nature (London)* **280**, 794 (1979).
3. M. A. Uman, *Lightning* (McGraw-Hill, New York, 1969).
4. F. L. Scarf, D. A. Gurnett, W. S. Kurth, *Science* **204**, 991 (1979).
5. D. A. Gurnett, R. R. Shaw, R. R. Anderson, W. S. Kurth, F. L. Scarf, *Geophys. Res. Lett.* **6**, 511 (1979).
6. R. Helliwell, *Whistlers and Related Ionospheric Phenomena* (Stanford Univ. Press, Stanford, Calif., 1965).
7. J. W. Warwick *et al.*, *Science* **204**, 995 (1979).
8. J. D. Menietti and D. A. Gurnett, *Geophys. Res. Lett.* **7**, 49 (1980).
9. P. Stone, in *Jupiter*, T. Gehrels, Ed. (Univ. of Arizona Press, Tucson, 1976), p. 586.
10. E. T. Pierce, in *Lightning*, R. H. Golde, Ed. (Academic Press, New York, 1977), p. 351.
11. R. L. Kirkwood, *NASA RM-4417* (1965).
12. D. J. Malan, *Physics of Lightning* (English Universities Press, London, 1963).
13. S. J. Weidenschilling and J. S. Lewis, *Icarus* **20**, 465 (1973); G. E. Hunt, *Mon. Not. R. Astron. Soc.* **161**, 347 (1973); J. S. Lewis, *Icarus* **10**, 365 (1969).
14. J. S. Lewis, *Icarus* **43**, 85 (1980).
15. D. Strobel, *J. Atmos. Sci.* **30**, 489 (1973).
16. R. G. Prinn, *Icarus* **13**, 424 (1970).
17. J. S. Lewis and R. G. Prinn, *Science* **169**, 472 (1970).
18. R. G. Prinn and J. S. Lewis, *ibid.* **190**, 294 (1975).
19. I thank the NASA Planetary Atmospheres Program for support of this research under grant NGL-22-009-521.

22 July 1980

Fluoride Distribution and Biological Availability in the Fallout from Mount St. Helens, 18 to 21 May 1980

Abstract. Concentrations of fluoride in the ash fallout in central Washington from the 18 May 1980 eruption of Mount St. Helens varied severalfold, but none are high enough to constitute any immediate hazard to animal life. The heaviest fallout (Moses Lake) contained 113 parts per million (ppm) of acid-labile fluoride, but of this only 11 ppm was water-soluble and 20 ppm was available to rats. The fluoride concentrations in the urine of cattle feeding for 4 days on hay contaminated with this ash were essentially normal. Samples of ash from other areas generally had higher concentrations of acid-labile fluoride but lower concentrations of water-soluble fluoride. The concentration of water-soluble fluoride was inversely correlated with the coarseness of the fallout.

The distribution and biological availability of fluoride in the ash from Mount St. Helens are of interest since some volcanic ash has caused heavy loss of livestock as a result of fluorosis (1). Stoiber *et al.* reported that the ash that fell on 4 and 12 April 1980 contained 8 parts per million (ppm) of fluoride (2). This concentration, which corresponds to the wa-

ter-soluble fraction (3), is not alarming, but it is not known whether water-soluble fluoride is the only form that is biologically important or whether the concentrations vary. In an effort to shed some light on these questions, I carried out preliminary experiments on ash samples collected from central Washington after the large eruption of Mount St.

Helens on 18 May 1980. Since most animals have acidic gastric secretions, acid-labile as well as water-soluble fluoride determinations were made on the ash samples. Multiple water extractions were carried out to determine whether more than one was necessary. I determined the biologically available fluoride by measuring the increase in urinary fluoride with the addition of ash to the diet. Standardization of the relationship between urinary fluoride and absorbed fluoride was done by adding NaF to the diet.

Twelve samples of ash were collected from 11 widely scattered sites between 19 and 21 May (Fig. 1). The major eruption occurred on 18 May, and fallout continued through the sampling period. Samples 1 through 8 were collected between 8 a.m. and 3:15 p.m. on 20 May when the road from Richland to Quincy was opened temporarily. Approximately 50 g of ash was collected at each site from the full thickness of the deposit on bridge rails or other objects likely to have been reasonably clean prior to the deposition of fallout. Sample 12 was collected 24 hours later from sample site 8, a patio that had been washed down after the first collection. No rain fell in the area until late on 21 May (4), after the samples had been collected. The ash material ranged from fine, dark sand to very fine, buff-colored powder. Samples from the south and west were generally coarser than the others. Visual ranking of coarseness and estimates of fallout depth are listed along with extraction methods, pH, and fluoride concentrations in Table 1. Multiple extractions with water resulted in the solubilization of about 50 percent more fluoride, an indication that some fluoride is slowly released or is bound to the particles.

There was an eightfold variation in the water-soluble fluoride by sample site, regardless of the extraction method used. The coarser samples contained less water-soluble fluoride. Regression analysis in which coarseness rankings were used as the independent variable and the multiply extracted, water-soluble fluoride concentrations were used as the dependent variable showed that 71 percent of the variability in the latter was explainable by this crude estimate of particle size.

Considerably more fluoride could be obtained from the samples by prolonged diffusion over several days of the fluoride from acidified suspension of the ash. These values ranged from 77 to 210 ppm and showed a relatively low correlation with water-soluble concentrations (correlation coefficient $r = .40$).

In order to learn which fluoride value

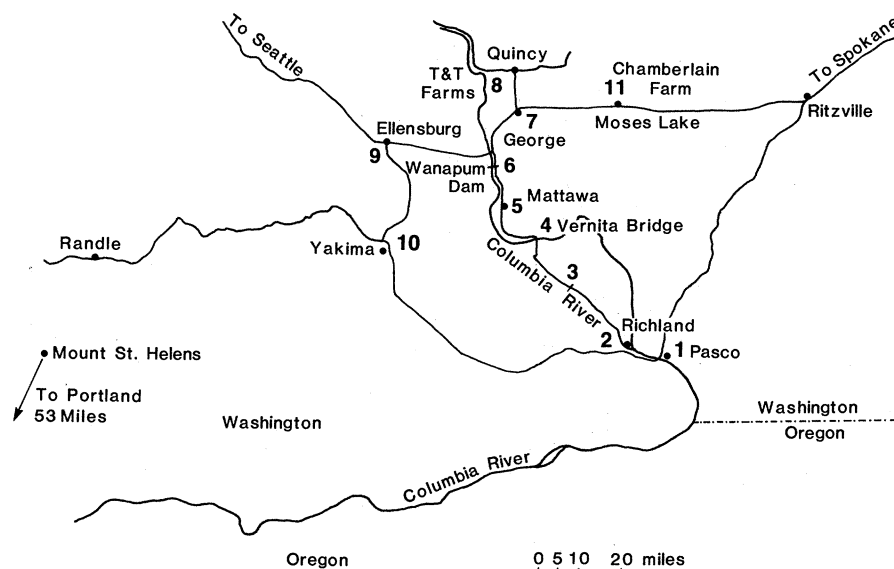


Fig. 1. Sample sites in central Washington.

most closely approximated the biological risk, one of the samples (from site 11) was fed to rats. I used this sample because it arrived first and was accompanied by urine specimens from cows feeding on hay contaminated with this ash. This sample also represented the most potential hazard on the basis of water solubility and depth of fallout. The ash was mixed with low-fluoride rat Chow (Tekland) that had been ground to powder form. The rats received plain diet for 2 days before the first 24-hour control period in order to reduce and stabilize the urine fluoride. To avoid contamination of urine with spilled food, the rats were placed in clean metabolic cages and limited to distilled water intake after a 6-hour feeding period each day. The

average fraction of fluoride recovered from the urine in excess of the three control periods was 22.5 percent when 12.3 ppm of fluoride as NaF was added to the diet. On the assumption that the same figure would apply to the fluoride absorbed from the ash, it is possible to calculate the amount of absorbable fluoride present in the ash. The increase in urinary fluoride with the ash (one part to ten parts of food) was about 50 percent greater than the average for three control periods. The calculated amount of absorbable fluoride in the ash eaten by each rat in three 24-hour periods was 20.5 ± 2.5 ppm, that is, about twice the amount estimated to be present as water-soluble fluoride.

This amount of biologically available

Table 1. Characteristics and fluoride concentrations of ash. Extraction method 1: 1-hour shaking of 1 g of ash in 5 ml of distilled water followed by centrifugation for 10 minutes; method 2: same as method 1 except with three additional water extractions; method 3: diffused from ash with hexamethyldisiloxane-saturated 1.5N HCl as described in (8). The values from the two consecutive 3-day diffusion periods were added. Each number is the average of two determinations with less than 10 percent disagreement.

Sample	Coarseness*	Estimated† depth (mm)	pH‡	Water-soluble (ppm)		Acid-diffused (ppm), method 3
				Method 1	Method 2	
1	1	1	6.4	1.27	2.13	123
2	2	2	6.1	1.35	1.77	123
3	9	3	5.5	3.50	5.86	160
4	5	3	5.6	3.59	4.82	129
5	4	15	5.9	3.27	5.06	102
6	11	25	6.2	5.96	8.06	122
7	7	40	6.3	5.16	8.12	126
8	6	12	6.2	4.68	7.60	190
9	10	10	6.4	3.27	5.67	231
10	3	15	6.0	2.69	3.57	77
11	12	50	6.3	7.33	11.6	113
12	8	4	6.6	9.94	14.6	210

*Visual estimate from the size and flow characteristics in a rotating tube.

†Visual estimate made while taking samples.

‡Average pH measurements on supernatants treated according to method 1.

fluoride is too low to constitute a significant hazard to animals. This conclusion is supported by the finding that only 3 to 6 ppm of fluoride was present in the urine of the cows which had been eating contaminated hay for 4 days. The normal urinary fluoride for cattle is age-dependent, and only one of the four specimens was higher than the limit set by Shupe (5). A 10 percent contamination of hay would raise the absorbable fluoride by only 2 ppm, which is about one-fifth of the amount that Shupe considers normal for hay and one-twentieth of the amount allowed in Washington State for a yearly weighted average (6).

There are, however, some additional points that need clarification. The higher concentration of water-soluble fluoride in the finer fallout samples suggests that ash from areas farther away from Mount St. Helens would have higher water-soluble fluoride concentrations. Analyses from such samples would be of interest. The ash collected from site 8 on 21 May showed twice as much water-soluble fluoride as the earlier material. Therefore, it would seem desirable to monitor fluoride concentrations in ash from future eruptions. Further work seems desirable to develop a chemical measurement that more accurately reflects the biologically available fluoride. The relationship between particle size and the amount of water-soluble fluoride is consistent with earlier findings (1) and appears to be reasonable in light of the encrustation of soluble material during volcanic eruptions (7). Individuals who would like to make additional measurements may obtain gram quantities of the above samples by writing to the author.

DONALD R. TAVES

Department of Pharmacology and
Toxicology, University of Rochester
School of Medicine and Dentistry,
Rochester, New York 14642

References and Notes

1. S. Thorarinsson, *Kekla: A Notorious Volcano*, J. Hannesson, Transl. (Almenna Bokafelagid, Reykjavik, Iceland, 1970), pp. 46-48.
2. R. E. Stoiber, S. N. Williams, L. L. Malinconico, *Science* **208**, 1258 (1980).
3. R. E. Stoiber, personal communication.
4. As documented by the U.S. Weather Service, Yakima, Wash.
5. F. L. Shupe, *Int. Tag. Weltges. Buiatrik* **4**, 1 (1966).
6. F. A. Smith and H. C. Hodge, *Crit. Rev. Environ. Control* **9**, 1 (1979).
7. W. I. Rose, *Geology* **5**, 621 (1977).
8. C. Waterhouse, D. R. Taves, A. Munger, *Clin. Sci.* **58**, 145 (1980).
9. I wish to thank Richard Carol and Kenneth Toews, Marion Chamberlain, and James Milton for collecting ash samples. This work was supported in part by a center grant (ES 01247) from the National Institute of Environmental Sciences.

7 July 1980; revised 15 August 1980

Deforestation and Increased Flooding of the Upper Amazon

Abstract. *The height of the annual flood crest of the Amazon at Iquitos has increased markedly in the last decade. During this same period, there has been greatly increased deforestation in the upper parts of the Amazon watershed in Peru and Ecuador, but no significant changes in regional patterns of precipitation. The change in Amazonian water balance during the last decade appears to be the result of increased runoff due to deforestation. If so, the long-predicted regional climatic and hydrological changes that would be the expected result of Amazonian deforestation may already be beginning.*

The Amazon is the world's greatest river (1, 2). One of the most striking aspects of the Amazonian water balance is the marked seasonal fluctuation in water level of the upper Amazon and its major tributaries in synchrony with the differential precipitation of the region's wet and dry seasons. The annual difference between high and low water levels may reach 20 m, and life in the Amazon basin is intimately related to the predictable annual flood cycle (2).

Although Amazonia remains by far the largest area of tropical forest on earth, it is being subjected to the same rapid ravages of deforestation as the rest of the world's tropical forests (3, 4). Perhaps as much as a fifth or a fourth of the Amazonian forest has already been cut (3, 4) and the rate of forest destruction is accelerating. Until recent years, most of this deforestation had been concentrated in lower Amazonia, especially in the region of Belem. However, opening of new

roads across the Andes, especially in the last decade, has led to settlement of large new areas of upper Amazonian Bolivia, Peru, Ecuador, and Colombia. During the last decade the population of Amazonian Peru has doubled (3, 5) and that of Amazonian Ecuador more than doubled from 1962 to 1974 (3, 6). This rapid increase in population has been accompanied by large-scale deforestation all along the base of the Andes; 51,000 km² of Peruvian Amazonian forest has been destroyed, mostly in the last decade (3, 5). The Valley of the Huallaga, opened by construction of the Carretera Marginal, is now almost completely deforested. Similarly large areas of the upper Marañon have been deforested, mostly subsequent to construction of the new oil pipeline and access road. The Apurimac Valley was mostly virgin forest in 1968, but has now been virtually clear-cut (7). The same pattern is prevalent in Ecuador where the expanding strip of newly cleared and settled land at the base of the Andean foothills is obvious on the map of the country's remaining forests developed by the Food and Agriculture Organization (8).

Extensive deforestation has been linked to major climatological and hydrological changes (9). In Venezuela, for example, deforestation of the south slopes of the coastal cordillera and northeasternmost Andean spur has led to loss of water retention capacity and more rapid runoff. Streams draining this region which formerly were continually flowing across the llanos now dry up during the dry season (10). With reference to Amazonia, Saletti and his co-workers (11) have shown that about half of the precipitation of the entire Amazonian basin results from water recycled by transpiration, and Sioli (12) has emphasized that the volume of runoff leaving Amazonia at the mouth of the Amazon or entering it via the tradewinds is only a fraction of the volume of water continually recycled through transpiration and rainfall in the Amazon basin. Extensive deforestation would be expected to greatly reduce the transpired water available for rainfall and might eventually convert

Table 1. Annual high and low water levels of the Amazon at Iquitos, 1962 to present; N.S., not significant.

Year*	High (m)	Low (m)
1962	25.82	18.24
1963	25.35	16.50
1964	24.29	20.26
1965	24.05	20.97†
1966	24.89	19.43
1967	25.35	19.31
1968	25.23	20.85
1969	25.06	19.54
1970	27.13	20.49
1971	27.36	21.91
1972	26.65	22.51
1973	27.13	18.81
1974	27.49	19.42
1975	27.08	19.10
1976	27.51	18.80
1977	27.54	18.80
1978	26.21	17.57
\bar{X} (1962-1969)	25.0 ± .6	19.4 ± 1.4
\bar{X} (1970-1978)	27.1 ± .4	19.7 ± 1.6
	$t = 3.4274$,	N.S.
	$P < .001$	

*Data from 1962 to 1972 were extracted from (19). Data from 1972 to the present were extracted from original records by C. Diaz and H. de Diaz. †Year began with an even lower peak because of prolonged low water of previous year.